Available online at www.elixirpublishers.com (Elixir International Journal)

Corrosion and Dye

Elixir Corrosion & Dye 87 (2015) 35501-35510

ISSN: 2229-712X

Corrosion Inhibition of Mild Steel Using Pluchea Dioscoridis (L) in Hydrochloric Acid Environment

A.S. Fouda[1], R.M. Abou shahba[2], A.El.El-Shenawy[2] and A.S. Mohamed[1]

[1] Department of Chemistry, Faculty of Science, El-Mansoura University, El-Mansoura-35516, Egypt, Fax: +2 0502246254

[2]Department of Chemistry, Faculty of Science, El-Azhar University, Nasr city, Egypt.

ARTICLE INFO

Article history:

Received: 1 September 2015;

Received in revised form:

23 September 2015;

Accepted: 29 September 2015;

Keywords

PDE,

EIS,

EFM,

SEM.

ABSTRACT

Anticorrosion activity of Pluchea dioscoridis (L) extract (PDE) as a corrosion inhibitor for mild steel in 1M HCl has been investigated using mass loss, potentiodynamic polarization, electrochemical impedance spectroscopy (EIS), scanning electron microscopy (SEM). The mass loss results show that PDE is an excellent corrosion inhibitor. The inhibition efficiency increases with increasing the temperature from 25 to 45°C, reaching a maximum value of 82 % at the highest concentration of 300 ppm at the temperature of 45°C. Polarization measurements demonstrate that the PDE acts as a mixed type inhibitor. Nyquist plot illustrates that on increasing PDE concentration, the charge transfer resistance increases and the double layer capacitance decreases. The adsorption of PDE on mild steel obeys Temkin adsorption isotherm. SEM studies confirm the adsorption of PDE on mild steel surface.

Introduction

Iron and its alloys play crucial roles in our daily lives due to their excellent properties, such as high structural and mechanical strengths [1, 2]. These materials are used in various industrial and engineering applications. Acid solutions are widely used for the removal of rust and scale in several industrial processes such as acid pickling, chemical and electrochemical etching, industrial acid cleaning, cleaning of oil refinery equipment, oil well acidizing and acid descaling, resulting in huge economic losses and many potential safety questions due to metallic corrosion[3,4]. The use of inhibitors is one of the most practical methods for protection against corrosion [5, 6], particularly in acidic media [7]. Different organic and inorganic inhibitors have been used in prevention methods. These compounds have shown good anticorrosive activity but most of them are highly toxic to both human beings and the environment. Such inhibitors may cause reversible (temporary) or irreversible (permanent) damage to organ system viz., kidneys or liver, or to interrupt a biochemical process or to disturb an enzyme system at some site in the body. The toxicity may manifest either during the synthesis of the compound or during its applications. Although the most effective and efficient organic inhibitors are compounds that have π bonds, the biological toxicity of these products, especially organic phosphate, is documented specifically about their environmental harmful characteristics [8]. The safety and environmental effects of corrosion inhibitors in industries have been always a global concern. Currently the use of natural products as corrosion inhibitor is gaining momentum to protect the metal against corrosion in aggressive acid solution. From the standpoint of safety, the development of non-toxic and effective inhibitors is considered more important and desirable, nowadays, which are also called eco-friendly or green corrosion inhibitors [9, 10]. These toxic effects have led to the use of natural products as anticorrosive agents which are eco-friendly and harmless. In recent days many alternative eco-friendly corrosion inhibitors have been studied [11].

In this work, a plant extract called Pluchea dioscoridis (L) is a wild growing highly branched shrub that attains a height of one to three meters and is characterized by being hairy and glandular. The plant is widely distributed in the Middle East and surrounding African countries. In Egypt, it occurs mainly in Nile region, Western and Eastern Deserts, Sinai Peninsula and Oases of the Mediterranean coastal strip [12]. Pluchea dioscoridis is reputed in folk medicine as a popular remedy to relieve rheumatic pains [13] as well as, carminative and in treatment of epilepsy in children, colic, ulcer and cold [14]. Farmers in Egypt call Pluchea dioscoridis "mosquito tree" due to its insect repellent effect [15]. Scientifically-based bioactivity studies proved that Pluchea dioscoridis extract exhibited (among those of other Egyptian medicinal plants) a significant anti-diarrheal activity, a diuretic, anti-hyperglycemic, anti-ulerogenic, antimicrobial, anti-inflammatory, ant nociceptive and antipyretic effects [16 -18]. In addition to a diuretic effect [19] furthermore, the volatile constituents of Pluchea dioscoridis showed promising antimicrobial activities and the extract of the combined aerial parts possessed anti-inflammatory activity [20] .However, nothing could be traced concerning either the constituents of the roots or its antihyperglycemic activity.

In the present study, the adsorption and the corrosion inhibition effect of PDE has been investigated using chemical and electrochemical techniques. Also, surface morphology was tested using scanning electron microscopy (SEM).

Experimental methods

Mild steel sample

Mild steel with chemical composition (weight %) Fe 99.77, C 0.064, Si 0.020, Mn 0.110, P 0.0044, Ni 0.0043, Al 0.025, Cu 0.0209, S 0.003, Ti 0.001 Co 0.0039, Mo 0.00167 was used for all measurements and surface analysis.

Test solutions

The solution of 1M hydrochloric acid (Test solution) were prepared for each experiment using analytical grade of hydrochloric acid (37%) and diluted with distilled water from

Tele:

E-mail addresses: asfouda@hotmail.com

the standard 6 M HCl solution. The concentration range of inhibitor was 50 to 300 ppm.

Preparation of plant extracts

Fresh aerial parts of Pluchea dioscoridis (L) sample were crushed to make fine powder. The powdered materials (250 g) were soaked in 500 ml of dichloromethane for 5 days and then subjected to repeated extraction with 5× 50 ml until exhaustion of plant materials. The extracts obtained were then concentrated under reduced pressure using rotary evaporator at temperature below 50°C. The dichloromethane evaporated to give solid extract that was prepared for application as corrosion inhibitor. Several compounds were reported in the literature which were isolated from methanol extract of Pluchea dioscoridis such as flavonoids, steroids, and sesquiterpenoids [21]. Thirteen compounds were also reported such as cholesterol (**1**), β-sitosterol (**2**), α-amyrin (**3**), conyzin (**4**), lupeol acetate (**5**), β-sitosterolglucoside (**6**), gallic acid (**7**), *p*-caffeic acid (**8**), syringic acid (**9**), rutin (**10**), quercitrin (**11**), quercitin (**12**) and kaempferol (**13**). Compounds (**6**) and (**8**) are newly reported in the species [53].

Weight lose measurements

Seven parallel mild steel sheets of 2×2×0.1 cm were abraded with emery paper (grade 320 to1200grit size) and then washed with bidistilled water and acetone. After accurate weighting, the specimens were immersed in a 100 ml beaker, which contained 100 ml of HCl with and without addition of different concentrations of PDE. All the aggressive acid solutions were open to air. After 180 minutes, the specimens were taken out, washed, dried, and weighted accurately. The average weight loss of seven parallel mild steel sheets could be obtained. The inhibition efficiency (IE %) and the degree of surface coverage θ of PDE for the corrosion of mild steel were calculated as follows [22]

$$\%IE = \theta x100 = [1-(W/W^{o})] \times 100 \quad (1)$$

Where W^{o} and W are the values of the average weight losses without and with addition of the inhibitor, respectively.

Electrochemical measurement

A three-electrode cell including a working electrode, an auxiliary electrode and a reference electrode was used for the electrochemical measurements. The working electrodes were made of mild steel sheets which were embedded in PVC holder using epoxy resin with a square surface of 1 cm^2.The auxiliary electrode was a platinum foil, the reference electrode was a saturated calomel electrode (SCE) with a fine Luggin capillary tube positioned close to the working electrode surface in order to minimize ohmic potential drop (IR). Each specimen was successive abraded by using SiC emery papers up to 1200 grit size, washed with bidistilled water and degreased in acetone then dried between filter papers. The working electrode was immersed in the test solution at open circuit potential for 30 min before measurement until a steady state reached. All the measurements were done in solutions open to atmosphere under unstirred conditions. All potential values were reported versus PDE. Prior to each experiment, the electrode was treated as before. Tafel polarization curves were determined by polarizing to ± 250 mV with respect to the free corrosion potential (E vs. SCE) at a scan rate of 0.5 mV/s. Stern-Geary method [23] used for the determination of corrosion current is performed by extrapolation of anodic and cathodic Tafel lines to a point which gives log i_{corr} and the corresponding corrosion potential (E_{corr}) for inhibitor free acid and for each concentration of inhibitor. Then i_{corr} was used for calculation of inhibition efficiency (%IE) and surface coverage (θ) as in equation 2:

$$\%\ IE = \theta \times 100 = [1- (i_{(inh)} / i_{(free)})] \times 100 \quad (2)$$

Where $i_{corr(free)}$ and $i_{corr(inh)}$ are the corrosion current densities in the absence and presence of inhibitor, respectively.

Electrochemical impedance spectroscopy measurements EIS were carried out in a frequency range of 100 kHz to 100 mHz with amplitude of 5 mV peak-to-peak. . The experimental impedance was analyzed and interpreted based on the equivalent circuit. The main parameters deduced from the analysis of Nyquist diagram are the charge transfer resistance R_{ct} (diameter of high-frequency loop) and the double layer capacity C_{dl}. The inhibition efficiencies and the surface coverage (θ) obtained from the impedance measurements are calculated from equation 3:

$$\%IE = \theta x100 = [1-(R^{o}_{ct}/R_{ct})] \times 100 \quad (3)$$

Where R^{o}_{ct} and R_{ct} are the charge transfer resistance in the absence and presence of inhibitor, respectively.

Electrochemical frequency modulation EFM, was carried out using two frequencies 2 and 5 Hz. The base frequency was 0.1 Hz, so the waveform repeats after 1 s. The higher frequency must be at least two times the lower one. The higher frequency must also be sufficiently slow that the charging of the double layer does not contribute to the current response. Often, 10 Hz is a reasonable limit. The Intermodulation spectra contain current responses assigned for harmonical and intermodulation current peaks. The large peaks were used to calculate the corrosion current density (i_{corr}), the Tafel slopes (β_a and β_c) and the causality factors CF-2&CF-3 [24]. The electrode potential was allowed to stabilize 30 min before starting the measurements. All the experiments were conducted at 25°C

All electrochemical measurements were performed using Gamry Instrument (PCI4/750) Potentiostat/Galvanostat/ZRA. This includes a Gamry framework system based on the ESA 400. Gamry applications include DC105 software for potentiodynamic polarization, EIS 300 software for electrochemical impedance spectroscopy, and EFM 140 software for electrochemical frequency modulation measurements via computer for collecting data. Echem Analyst 6.03 software was used for plotting, graphing, and fitting data. To test the reliability and reproducibility of the measurements, duplicate experiments, which performed in each case at the same conditions.

Scanning Electron Microscopy (SEM)

The mild steel specimens were immersed for 12 h in 1M HCl solution containing optimum concentrations (300 ppm CDE) of inhibitor. After 12 h, the specimens were taken out and dried. Examination of mild steel surface after 12 h exposure to 1 M HCl solution without and with inhibitor was carried by using (JEOL JSM-5500) scanning electron microscope.

Results and Discussion

Weight loss measurements

Weight loss measurements were carried out for mild steel in 1M HCl in the absence and presence of different concentrations of PDE are shown in Figure (1). The inhibition efficiency (IE %) values calculated are listed in Table 1, From this table, it is noted that the IE% increases steadily with increasing the concentration of CDE and surface coverage (θ)were calculated by equation (1).

The observed inhibition action of the PDE could be attributed to the adsorption of its components on mild steel surface. The formed layer, of the adsorbed molecules, isolates the metal surface from the aggressive medium which limits the dissolution of the latter by blocking of their corrosion sites and hence decreasing the corrosion rate, with increasing efficiency as their concentrations increase [25].

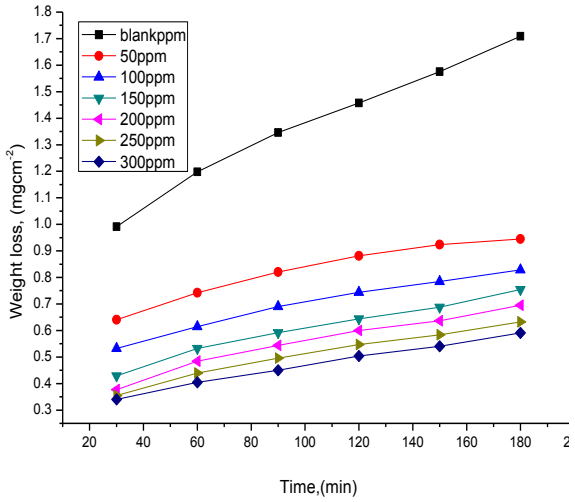

Figure 1. Weight loss-time curves for the corrosion of mild steel in 1 M HCl in the absence and presence of different concentrations of PDE at 25°C

Electrochemical impedance spectroscopy (EIS) measurements

The corrosion behavior of mild steel in 1 M HCl solution in the presence of PDE was investigated by EIS at 25°C after 30 min of immersion. Figure 2 shows the results of EIS experiments in the Nyquist representation. After analyzing the shape of the Nyquist plots, it is concluded that the curves approximated by a single capacitive semi-circles, showing that the corrosion process was mainly charge transfer controlled [26]. The general shape of the curves is very similar for all samples; the shape is maintained throughout the whole concentrations, indicating that almost no change in the corrosion mechanism occurred due to the inhibitor addition [27].The diameter of Nyquist plots (R_s) increases on increasing the PDE concentration. These results suggest the inhibition behavior of PDE on corrosion of mild steel in 1 M HCl solution.

The Nyquist plots are analyzed in terms of the equivalent circuit composed with classic parallel capacitor and resistor (shown in Figure 3) [28].The impedance of a CPE is described by the equation 4:

$$Z_{CPE} = Y_0^{-1} (j\omega)^{-n} \quad (4)$$

where Y_0 is the magnitude of the CPE , j is an imaginary number, ω is the angular frequency at which the imaginary component of the impedance reaches its maximum values and n is the deviation parameter of the CPE: $-1 \leq n \leq 1$. The values of the interfacial capacitance C_{dl} can be calculated from CPE parameter values Y_0 and n using equation 5:

$$C_{dl} = Y (\omega_{max})^{n-1} \quad (5)$$

The impedance parameters including polarization resistance R_{ct}, double layer capacitance C_{dl} and inhibition efficiency % IE are given in Table

Also, Bode plots for the mild steel in 1 M HCl solution are shown in Figure (4). In which the high frequency limit corresponding to the electrolyte resistance (ohmic resistance) R_Ω, while the low frequency represents the sum of (R_Ω + R_{ct}), where R_{ct} is in the first approximation determined by both electrolytic conductance of the oxide film and the polarization resistance of the dissolution and repassivation process. At both low and high frequency limits, the phase angle between the current and potential (θ), assumes a value of about 0°, corresponding to the resistive behavior of R_Ω and (R_Ω + R_{ct}).

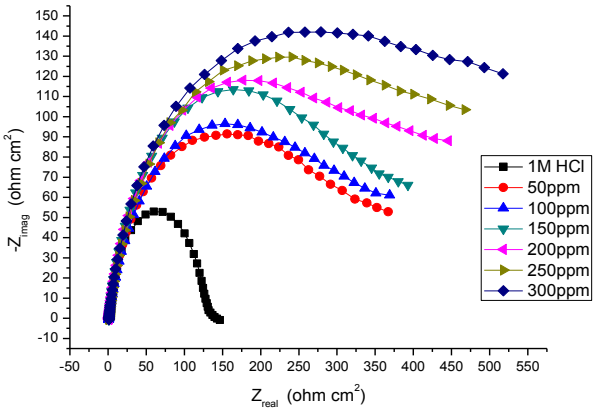

Figure 2. Nyquist plots for mild steel in 1M HCl at different concentrations of PDE

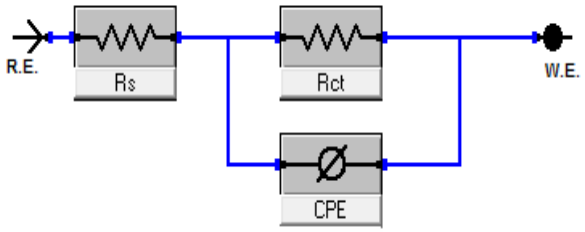

Figure 3. Electrical equivalent circuit used to fit the impedance data

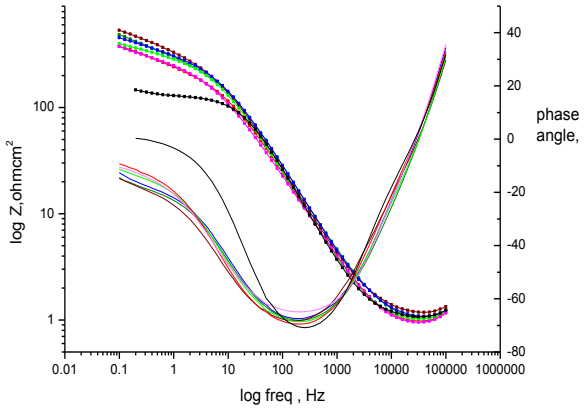

Figure 4. Bode plots for mild steel in 1M HCl solutions in the absence and presence of various PDE concentrations at 25°C

The main parameters deduced from the analysis of Nyquist diagram are:

- The resistance of charge transfer R_{ct}(diameter of high frequency loop)
- The capacity of double layer C_{dl} which is defined as :

$$C_{dl} = \frac{1}{2\pi R_{ct} f_{max}} \quad (6)$$

Where f_{max} is the maximum frequency at which the Z_{imag} of the impedance is a maximum. Since the electrochemical theory assumed that ($1/R_{ct}$) is directly proportional to the capacity of double layer C_{dl}, the inhibition efficiency (%IE) of the inhibitor for mild steel in 1 M HCl solution was calculated from R_{ct} values obtained from impedance data at different inhibitor concentrations from the following equation:

$$\%\, IE = \left(1 - \frac{R_{ct}^{\circ}}{R_{ct}}\right) \times 100 \quad (7)$$

Where R^{o}_{ct} and R_{ct} are the charge transfer resistance in the absence and presence of investigated extract, respectively.

It is clear that the value of R_{ct} increases on increasing the concentration of the inhibitor, indicating that the corrosion rate decreases in the presence of the inhibitor. It is also clear that the value of C_{dl} decreases on the addition of inhibitors, indicating a decrease in the local dielectric constant and/or an increase in the thickness of the electrical double layer, suggesting the inhibitor molecules function by the formation of the protective layer at the metal surface [29]. Deviations from a perfect circular shape indicate frequency dispersion of interfacial impedance. This anomalous phenomenon is attributed in the literature to the no homogeneity of the electrode surface arising from the surface roughness or interfacial phenomena [30, 31].

Potentiodynamic polarization measurements

Figure 5, represents the anodic and cathodic polarization curves of mild steel electrode, in 1 M HCl solutions containing different concentrations of PDE. Both anodic and cathodic polarization curves are shifted to less current density values in the presence of PDE. This behavior suggests the inhibitive action of PDE. The extent of the shift in current density increases with increasing of PDE concentration. The values of corrosion current density (i_{corr}), corrosion potential (E_{corr}), anodic Tafel constants (β_a) and cathodic Tafel constant (β_c), excluded from polarization curves are given in Table 3.

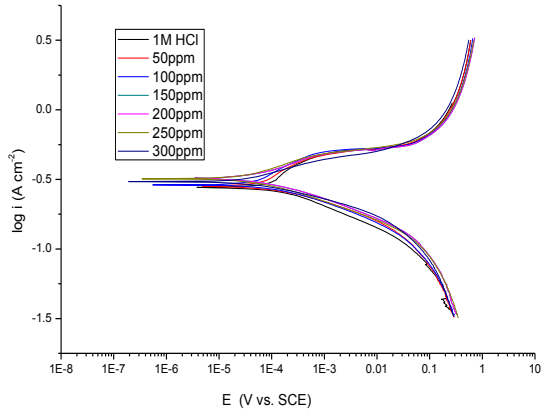

Figure 5. Potentiodynamic polarization curves for corrosion of mild steel in 1 M HCl in the absence and presence of different concentrations of PDE at 25°C

Inspection of Table 3 reveals that the corrosion potential of mild steel in the acid solution is largely shifted to less negative values (noble direction) upon addition of PDE. On the other hand, the corrosion current density is greatly reduced upon addition of PDE. These results suggest the inhibitive effects of the PDE. The data in Table 3 reveal that the values of inhibition efficiency obtained by polarization technique are comparable to those obtained by weight loss measurements and EIS. The inhibition efficiency increases with increasing PDE concentration. Further inspection of Table 3 reveals that the addition of increasing concentrations of PDE decreases both the anodic and cathodic Tafel constants. This result indicates that the PDE acts as mixed inhibitors [32] .This means that the PDE molecules are adsorbed on both the anodic and cathodic sites resulting in an inhibition of both anodic dissolution and cathodic reduction reactions. The greater the metal surface area occupied by adsorbed molecules, the higher the inhibition efficiency.

Electrochemical frequency modulation (EFM) measurements

EFM is a nondestructive corrosion measurement technique that can directly determine the corrosion current value without prior knowledge of Tafel slopes, and with only a small polarizing signal. These advantages of EFM technique make it an ideal candidate for online corrosion monitoring [33]. The great strength of the EFM is the causality factors which serve as an internal check on the validity of EFM measurement. The causality factors CF-2 and CF-3 are calculated from the frequency spectrum of the current responses. Figure 6 shows the frequency spectrum of the current response of mild steel in 1 M HCl solution, contains not only the input frequencies, but also contains frequency components which are the sum, difference, and multiples of the two input frequencies. The EFM intermodulation spectrums of mild steel in 1 M HCl solution containing (50- 300 ppm) of the PDE extract at 25°C is shown in Figure 6. The experimental EFM data were treated using two different models: complete diffusion control of the cathodic reaction and the "activation" model. For the latter, a set of three non-linear equations had been solved, assuming that the corrosion potential does not change due to the polarization of the working electrode [34]. The larger peaks were used to calculate the corrosion current density (i_{corr}), the Tafel slopes (β_c and β_a) and the causality factors (CF-2 and CF-3).These electrochemical parameters were simultaneously determined by Gamry EFM140 software, and listed in Table 4 indicating that this extract inhibit the corrosion of mild steel in 1 M HCl through adsorption. The causality factors obtained under different experimental conditions are approximately equal to the theoretical values (2 and 3) indicating that the measured data are verified and of good quality [35]. The inhibition efficiencies IE_{EFM} % increase by increasing the studied extract concentrations and was calculated as follows:

$$IE\ \%_{EFM} = \left(1 - \frac{i^{o}_{corr}}{i_{corr}}\right) \times 100 \quad (8)$$

Where i^{o}_{corr} and i_{corr} are corrosion current densities in the absence and presence of PDE extract, respectively.

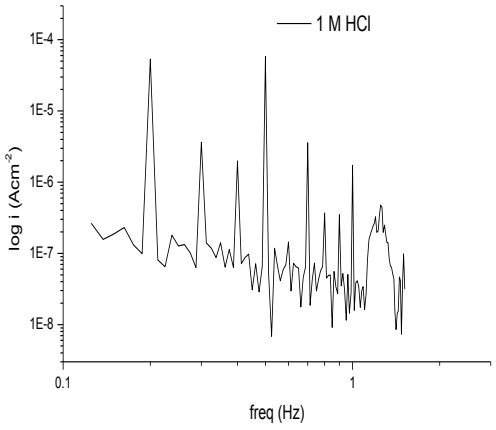

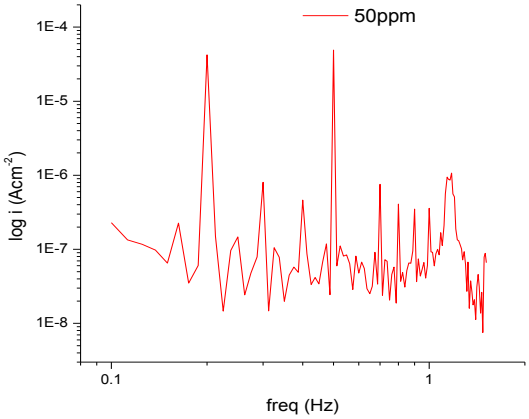

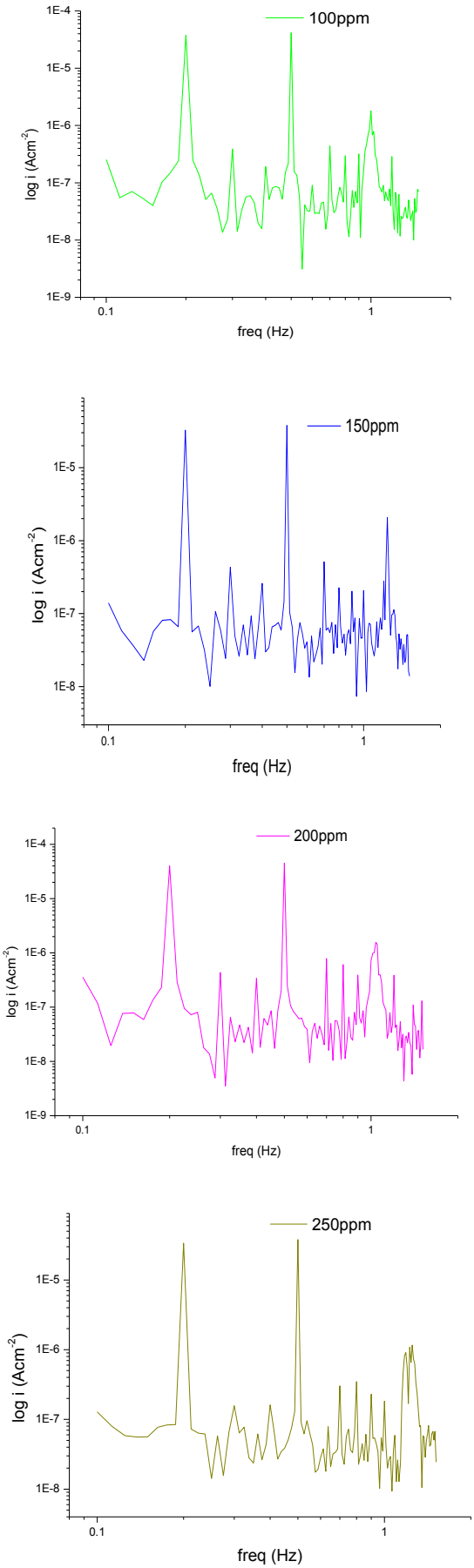

Figure 6. Intermodulation spectrums for the corrosion of mild steel in 1 M HCl without and with various concentrations of PDE at 25°C

Adsorption isotherms

Basic information on the interaction between inhibitors and metal surface can be provided using the adsorption isotherms [36].The adsorption of an organic molecules at metal–solution interface can occur as a result of substitution adsorption process between organic molecules presented in the aqueous solution (Org), and the water molecules previously adsorbed on the metallic surface (H_2O) [37]:

$$Org_{(sol)} + xH_2O_{(ads)} = Org_{(ads)} + xH_2O_{(sol)} \quad (9)$$

Where $Org_{(sol)}$ and $Org_{(ads)}$ are the organic species in the bulk solution and adsorbed one on the metallic surface, respectively H_2O is the water molecule adsorbed on the metallic surface and x is the size ratio representing the number of water molecules replaced by one organic molecule. The surface coverage values (θ) were evaluated using corrosion rate values obtained from the weight loss method. The (θ) values for different inhibitor concentrations were tested by fitting to various isotherms. The best fit was obtained with Temkin adsorption isotherm (Fig. 7), given by Eq. (10) [38].

$$\theta = 1/f \ln K_{ads}C \quad (10)$$

where f is the factor of energetic homogeneity, the heterogeneous factor of the metal surface describing the molecular interactions in the adsorption layer [39]. If $f > 0$, mutual repulsion of molecules occurs and if $f < 0$ attraction takes place [40]. In Figure 7 it can be seen that the linear correlation coefficient (R^2) is close to 1 and the slope of straight line is also close to 1, which suggests that the adsorption of PDE from 1 M HCl solution on mild steel obeys the Temkin model and exhibit single-layer adsorption characteristic. From the intercept of the straight line K_{ads} value can be calculated. The equilibrium constant of the adsorption process K_{ads}, is related to the standard free energy of adsorption, $\Delta G°_{ads}$, from the following equation [41]:

$$K_{ads}=1/55.5 \exp(\Delta G^0_{ads}/RT) \quad (11)$$

The value 55.5 is the concentration of water in solution in mol l^{-1}.The calculated ΔG^0_{ads}values, using Eq. (11), were also given in Table 5.

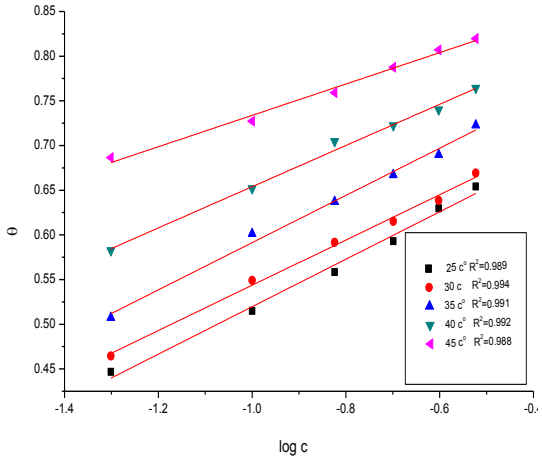

Figure 7. Temkin adsorption plots for mild steel in 1 M HCl containing various concentrations of PDE at 25°C

The negative values of ΔG^{o}_{ads} ensure the spontaneity of the adsorption process and the stability of the adsorbed layer on the steel surface. Early speaking, the adsorption type is regarded as physisorption if the absolute value of ΔG^{0}_{ads} was of the order of 20 kJ mol^{-1} or lowers. The inhibition behavior is attributed to the electrostatic interaction between the organic molecules and iron atom. With the absolute value of ΔG^{o}_{ads} is of the order of 40 kJ mol^{-1} or higher, the adsorption could be seen as chemisorption. In this process, the covalent bond is formed by the charge sharing or transferring from the inhibitor molecules to the metal surface [42, 43]. Based on the literature [44], the calculated ΔG^{o}_{ads} values in this work (Table 5) indicate that the adsorption mechanism of PDE on mild steel in 1 M HCl solution is typically chemisorption. The same conclusion was given by Wang et al. [45] and Hassan [46] .The large negative value of ΔG^{0}_{ads} of PDE indicates that this extract is strongly adsorbed on the steel surface [47-48].

Effect of temperature

The effect of temperature on the corrosion rate of mild steel in free acid and in the presence of different concentrations of PDE was studied in the temperature range of 25–45C^{O} using weight loss measurements. The corrosion rate values of mild steel with and without the addition of PDE extract in 1 M HCl at various temperatures are listed in Table 6. These data showed that the corrosion rate values decreased as the concentration and temperature of the PDE increased and hence the corrosion inhibition efficiency increased. This behavior was observed for chemisorption of inhibitors on metal surfaces.

Figure 8 represents Arrhenius plot (as log k versus 1/T) for mild steel corrosion in 1M HCl in the absence and presence of various concentrations of PDE. Straight lines were obtained with slope equals to E_a=2.303 R. The values of E_a for the corrosion reaction in the absence and presence of PDE were calculated and are presented in Table 6. In examining the effect of temperature on the corrosion process in the presence of the PDE, the Arrhenius equation below was used:

$$\text{Log } k = -E_a/2.303RT + \log A \qquad (12)$$

Where k is the corrosion rate, E_a is the apparent activation energy, and A is the frequency factor.

Table7.shows the decrease of E_a decelerated the corrosion rate of steel. E_a values of the corrosion process of protected mild steel are lower than the unprotected mild steel in 1 M HCl solution. The large decrease in the activation energy of the corrosion process in the presence of the inhibitor indicates the higher inhibition efficiency of the inhibitor. The decrease of the activation energy is due to the adsorption of inhibitor molecules on the metal surface to form stable metal-inhibitor complex (M Inh) [49].

The other thermodynamic parameters (ΔS^{*} and ΔH^{*}) were calculated from the linear regression of transition state (Fig.9) using Eq. (13)

$$k = (RT/Nh)\exp^{(\Delta S^{*}/R)}\exp^{(-\Delta H^{*}/RT)} \qquad (13)$$

Where k is rate of corrosion, h is Planck's constant, N is Avogadro number, ΔS^{*} is the entropy of activation and ΔH^{*} is the enthalpy of activation. A plot of log (k/T) vs. 1/T (Fig. 9) should give a straight line, with a slope of (ΔH^{*}/2.303R) and an intercept of [log (R/Nh)+ΔS^{*}/2.303R] Examination of the kinetic values shows that the increase of inhibitor concentration leads to increases of all parameters of corrosion process (Table 7). The positive value of the enthalpy ΔH^{*}) means that the process is endothermic and it needs more energy to achieve the activated state or equilibrium [50-51].The negative value of ΔS^{*} (Table 7) for PDE indicates that activated complex in the rate determining step represents an association rather than a dissociation step, meaning that a decrease in disorder takes place during the course of transition from reactant to the activated complex [52].

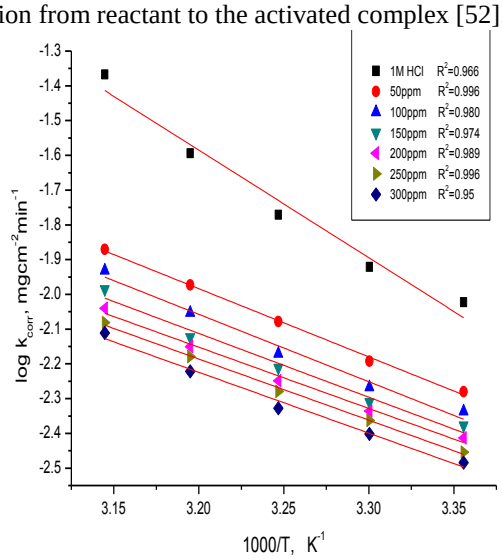

Figure 8. Log k (corrosion rate) – 1/T curves for mild steel in 1 M HCl in the absence and presence of different concentrations of PDE extract

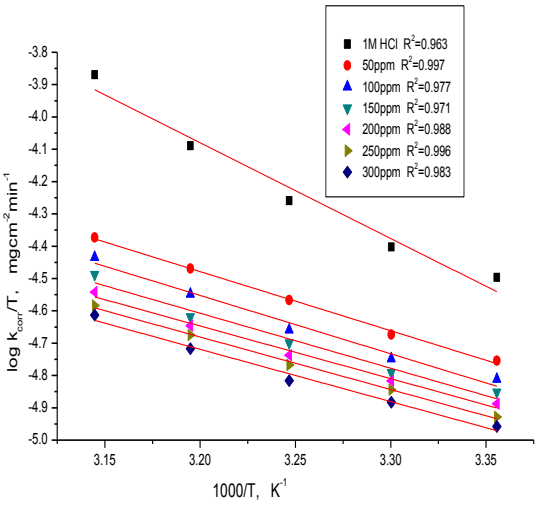

Figure 9. Log k (corrosion rate)/T – 1/T curves for mild steel in 1 M HCl in the absence and presence of different concentrations of PDE extract

Table 1. Corrosion rate (C.R.) in (mg cm^{-2} min^{-1}) and inhibition efficiency data obtained from weight loss measurements for mild steel in 1 M HCl solutions without and with various concentrations of PDE extract at 25°C

Conc., ppm	Weight loss mg cm^{-2}	C.R., mg cm^{-2} min^{-1}	Θ	% IE
1 M HCl	1.71	0.009	---	----
50	0.95	0.005	0.446	44.6
100	0.83	0.0046	0.515	51.5
150	0.75	0.004	0.558	55.8
200	0.70	0.0039	0.593	59.3
250	0.63	0.0035	0.630	63.00
300	0.59	0.0032	0.654	65.4

Table 2. EIS data of mild steel in 1 M HCl in the presence of different concentrations of PDE extract at 25° C

Conc., ppm	R_{ct}, Ωcm^2	C_{dl}, $x10^{-4}$ F cm^{-2}	Θ	% IE
1M HCl	129.4	68.9	-----	-----
50	294.8	1.481	0.561	56.1
100	306.6	1.321	0.578	57.8
150	335.3	1.31	0.614	61.4
200	367.9	1.162	0.648	64.8
250	373.7	1.149	0.653	65.3
300	435.5	1.072	0.702	70.2

Table 3. Potentiodynamic data of mild steel in 1 M HCl in the presence of different concentrations of PDE extract at 25°C

Conc., ppm	i_{corr}, μA cm^{-2}	$-E_{corr}$, mVvs.SCE	β_a, $mVdec^{-1}$	β_c, $mVdec^{-1}$	CR, mmy^{-1}	Θ	%IE
1M HCl	119.0	559	466.0	108.4	54.56	---	---
50	65.1	549	294.0	81.7	29.76	0.453	45.3
100	53.8	538	255.1	77.4	24.57	0.548	54.8
150	48.8	523	202.5	92.3	22.11	0.593	59.3
200	33.0	512	119.0	84.4	15.22	0.723	72.3
250	32.0	496	141.1	96.0	14.64	0.731	73.1
300	31.0	493	118.7	75.1	14.33	0.74	74.0

Table 4. Electrochemical kinetic parameters obtained by EFM technique for mild steel in the absence and presence of various concentrations of the PDE extract in 1 M HCl at 25ºC

Conc., ppm	i_{corr}, μA cm^{-2}	β_a $mV\ dec^{-1}$	β_c $mV\ dec^{-1}$	C.R. mpy	CF-2	CF-3	Θ	%IE
0.0	171.6	143.2	332.2	78.41	1.9	2.2	----	---
50	89.9	120	137	41.1	1.9	3.3	0.476	47.6
100	82.1	129.5	141.2	37.5	1.8	3.5	0.522	52.2
150	80.7	140.6	159.1	36.9	2.0	3.6	0.530	53.0
200	74.9	108.9	120.5	34.3	1.1	3.1	0.563	56.3
250	67.8	120.2	126.1	30.9	1.3	3.6	0.605	60.5
300	63.1	120.7	135.8	28.8	1.8	3.3	0.632	63.2

Table 5. Values of adsorption isotherm parameters for mild steel in 1 M HCl contain different concentrations of PDE extract

Temp., K	Adsorption isotherm	K_{ads}, $g^{-1}L$	$-\Delta G°_{ads}$, $kJ\ mol^{-1}$
298	Temkin	904.9	26.8
303		1400.5	28.4
308		1729.9	29.4
313		6847.5	33.4
315		151444.7	42.2

Table 6. Data of weight loss measurements for mild steel in 1 M HCl solution in the absence and presence of different concentrations of PDE extract at different temperatures

Conc., ppm	Temp., ^{o}C	C.R., mg cm^{-2} min^{-1}	Θ	% IE
50	25	0.005	0.447	44.7
	30	0.0064	0.464	46.4
	35	0.0084	0.507	50.7
	40	0.011	0.583	58.3
	45	0.014	0.687	68.7
100	25	0.0046	0.515	51.5
	30	0.0054	0.549	54.9
	35	0.0068	0.601	60.1
	40	0.0089	0.652	65.2
	45	0.0117	0.727	72.7
150	25	0.004	0.558	55.8
	30	0.0049	0.592	59.2
	35	0.0062	0.637	63.7
	40	0.0075	0.705	70.5
	45	0.0103	0.759	75.9
200	25	0.0039	0.593	59.3
	30	0.0046	0.615	61.5
	35	0.0056	0.667	66.7
	40	0.0071	0.722	72.2
	45	0.009	0.788	78.8
250	25	0.0035	0.63	63.0
	30	0.0043	0.639	63.9
	35	0.0053	0.69	69.0
	40	0.0066	0.74	74.0
	45	0.0083	0.807	80.7
300	25	0.0032	0.65	65.4
	30	0.004	0.669	66.9
	35	0.0047	0.723	72.3
	40	0.006	0.764	76.4
	45	0.0078	0.82	82.0

Table7. Activation parameters for dissolution of mild steel in the absence and presence of different concentrations of PDE extract in 1 M HCl at different temperatures

Conc., ppm	E_a kJ mol^{-1}	Δ H*, kJ mol^{-1}	-ΔS*, J $mol^{-1}K^{-1}$
1M HCl	59.3	24.6	94.2
50	37.6	15.2	171.2
100	37.1	15.0	174.1
150	35.1	14.1	181.5
200	33.8	13.5	186.7
250	33.7	13.5	187.6
300	33.5	13.4	188.8

Scanning electron microscope (SEM)

Figure 10 shows the SEM photos of mild steel surface in 1 M HCl. It can be seen from (Fig. 10 A) that the mild steel samples before immersion seems smooth and shows some abrading scratches on the surface. However, it also appears small black holes, which may be attributed to the defect of steel. The morphology in (Fig. 10B) shows the mild steel surface is damaged in some areas. Disclosing that in extract-free solution, the surface is highly corroded.

In case of mild steel immersed in 1M HCl solution with PDE, a smooth surface was noticed (Fig.10 C), showing less effective corrosion . In the of presence 300 ppm of PDE, there is much less damage on the steel surface, which further confirm the inhibition action. Also, there is an adsorbed film adsorbed on mild steel surface (Fig.10 C). In accordance, it might be concluded that the adsorption film can efficiently inhibits the corrosion of mild steel.

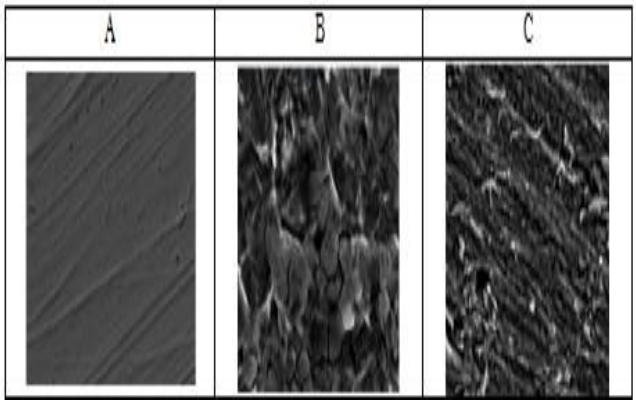

Figure 10. SEM micrographs of mild steel surface (10A) before of immersion in 1 M HCl, (10B) after 10 h of immersion in 1 M HCl and (10C) after 10 h of immersion in 1 M HCl+ 300 ppm PDE extract at 25°C

Conclusions

On the basis of this study the following conclusions can be drawn:

(1) PDE acts as inhibitor for mild steel corrosion in acidic medium.

(2) Inhibition efficiency of PDE increases with increase in concentration of the inhibitor and also with increase in temperature.

(3) The corrosion inhibition is probably due to the adsorption of the PDE on the metal surface and blocking its active sites by phenomenon of physical and chemical adsorption.

(4) PDE was found to obey Temkin adsorption isotherm from the fit of the experimental data at all the concentrations studied.

(5) The values of E^*_a obtained in the presence of the PDE were lower compared to the blank acid solution which further support the chemical adsorption proposed.

(6) The values of ΔG^o_{ads} obtained are low and negative, which reveals the spontaneity of the adsorption process

(7) SEM reveals the formation of a smooth surface on mild steel in presence of PDE probably due to the formation of an adsorptive film of electrostatic character.

(8) Also the results indicate that, the PDE acts as mixed type inhibitor.

References

[1] D.M. Strickland, Ind. Eng. Chem. 15 (1923) 566–569.
[2] J. D. Hatfield, A.V. Slack, G. L. Crow, H. B. Shaffer, J. Agric. FoodChem. 6 (1958) 524–531.
[3] B. Obot, N. O. Obi-Egbedi, Corros. Sci. 52 (2010) 198–204.
[4] H. Vashisht, I.Bahadur, S. Kumar, K. Bhrara, D. Ramjugernath, G. Singh, Int. J. Electrochem. Sci. 9 (2014) 2896–2911.
[5] N. Hackerman, doi:http://dx.doi.org/10.1021/la00078a009, 3 (1987) 922–924.
[6] P. G. Cao, J. L. Yao, J. W. Zheng, R. A. Gu, Z. Q. Tian, doi: 490 http://dx.doi.org/1 0.1021/la010575p, 18 (2002) 100–104,
[7] A. S. Fouda, A. M. Eldesoky, M. A. Elmorsi , M.Y. El sheik and I.A. El said, , Int. J. of Adva. Res. 2 (2014) 4-24
[8] M.A .Amee and A.M. Fekry, Prog Org. Coat., 71 (2011) 343.
[9] J.C.D. Rocha., J.A. Da Cunha Ponciano Gomes and E.D.Elia, Corros Sci., 52 (2010) 2341.
[10]M. Boudalia, A.Guenbour, A.Bellaouchou, A.Laqhaili and M.Mousaddak, Int J Electrochem Sci., 8 (2013) 7414.
[11]K.Parameswari, S.Rekha, S.Chitra and E.Kayalvizhy, Electrochem. Acta., 28 (2010) 4152.
[12] L. Boulos, Flora of Egypt. Al-Hadara Publishing: Cairo, 3 (2002)189.
[13] L. Boulos, and M. E1-Hadidi, the Weed Flora of Egypt. The American Univ. Cairo Press: Cairo; (1989) 361.
[14] I El Bitar, Mofradat Al AdwiahwalAghzia.Boulac Press: Egypt 11(1890).
[15] K.H.Shaltout, D.F. Slima. The biology of Egyptian woody perennials.Ass. Univ. Bull. Environ. Res., 10(2007) 85-103.
[16]A. Atta, Journal of Ethnopharmacology, 92 (2004) 303-309.
[17] M. E. Zain, A. S. Awaad, M. R. Al-Outhman, R. M. El-Meligy. Phytopharmacol, 2 (2012)106 – 113.
[18] S. M. Zalabani, M. H. Hetta, A. S. Ismail. Desf.Organs. Biosafety; 2 (2013) 106.
[19] A. Atta, Int. J. of Phar. and Pharmaceutical Sci., 2 (2010) 162-165.
[20] M. M. A. El-Hamouly, M.T. Ibrahim, Alex. J. of Phar. Sci., 17 (2003) 75-80.
[21] A. S. Awaad, R. M. El-meligy, S. A. Qenawy, A. H. Atta, G.A. Soliman. J Saudi Chem. Soc., 15 (2011) 367 – 373.
[23] G. N.Mu, T. P.Zhao, M.Liu, T.Gu, audi. Chem. Soc.; 15 (2011) 367 – 373.
[24] R. G.Parr, R. A.Donnelly, M.Levy, W. E. Palke, J. Chem. Phys., 68 (1978) 3801-3807.
[25] R. W.Bosch, J.Hubrecht, W. F.Bogaerts, B. C. Syrett, Corrosion, 57 (2001)60-70.
[26] D. Q.Zhang, Q. R.Cai, X. M.He, L. X. Gao, G. S.Kim,Mater. Chem. Phys. 114 (2009) 612.
[27] R. Rosliza, W. B.Wan Nik, H. B. Senin, Mater. Chem. Phys. 107 (2008) 281.
[28] F. M. Reisde, H. G. Melo; Costa, I., Electrochim. Acta. 51 (2006)1780.
[29] M. Abdel-Gaber, B .A. Abd-El-Nabey, I. M. Sidahmed, A.M.El-Zayaday, M. Saadawy, Corros. Sci. 48 (2006) 2765.
[30] A. Ostovari, S. M. Hoseinieh, M. Peikari, S. R. Shadizadeh, S.J.Hashemi, Corros.Sci. 51 (2009) 1935.
[31] M. A. Quraishi, I. H. Farooqi, P. A. Saini, Corrosion 55 (1999) 493.
[32] A. M. Abdel-Gaber, B. A. Abd-El-Nabey, M. Saadawy, Corros. Sci. 51 (2009) 1038.
[33] F. S. de Souza, A. Spinelli, Corros.Sci. 51 (2009) 642.
[34] E.Kus, F. Mansfeld, Corros. Sci., 48 (2006) 965.
[35] G. A. Caigman, S. K. Metcalf, E. M. Holt, J.Chem. Cryst, 30 (2000) 415.
[36] S. S. Abdel–Rehim, K. F. Khaled, N. S. Abd–Elshafi, Electrochim. Acta, 51 (2006) 3269.
[37] E. Naderi, A. H. Jafari, M. Ehteshamzadeh, and M. G. Hosseini, Mater. Chem. Phys. 113 (2009) 986–993.

[38] M. I. Temkin, J. Phys. Chem., 14(1940)1153.
[39] N. O. Obi-Egbedi, K. E. Essien and I. B. Obot, J. Comp. Method Mol. Design, 1(2011) 26-43.
[40] N. J. N. Nnaji, N.O. Obi-Egbedi and J. U. Ani, J. Sci. and Ind Studies, 9(2011) 26-32
[41] J. Flies, and T. Zakroczymski, J. Electrochem. Soc.143 (1996) 2458-2464.
[42] A. Yurt, S. Ulutas, and H. Dal, Appl. Surf. Sci. 253(2006) 919-925.
[43] F. Hongbo, Chemical Industry Press, Beijing, 103 (2002) 166.
[44] L. H. Wang, B.H. Fan, and S. J. Zheng, Mater. Chem. Phys. 77 (2003)655-661.
[45] H. H. Hassan, Electrochem.Acta. 53(2001)1722-1730.
[46] F. Bentiss, M. Lebrini, M. Lagrenée, M. A. Traisnel, A. Elfarouk, and H. Vezin, Electrochem.Acta. 52(2007)6865-6872.
[47] F. Bentiss, M. Traisnel, H.Vezin, F. H. Hildebrand, and M. Lagrenée, Corros. Sci. 46 (2004) 2781-2792.
[48] H. Ashassi-Sorkabi, N. Gahlebsaz-Jeddi, F. Hashemzadeh, and H. Jahani, Electrochem.Acta. 51(2006)3848–3855.
[49] M. Bouklah, N. Benchat, B. Hammouti, A. Aouniti, and S. Kertit, Mater. Lett. 60(2006)1901-1905.
[50] K. O.Orubite and N.C. Oforka, Mater.Lett. 58 (2004)1768-1772.
[51] M. HazwanHussin and M.Jain Kassim, Mater. Chem. Phys. 125(2011)461-468.
[52] V. Ramesh Saliyan, A. V. Adhikari, Bull, Mater. Sci. 31(2007)699–711.
[53] M. El Zalabani, H. Hetta, A. Ross Samir, M. Abo Youssef, Mohamed A. Zaki and S. Ismail Ahmed, Australian J. of Basic and Appl. Sci., 6(2012)257-265.